

# The tidal interaction between planets and the protoplanetary disk

Willy Kley

*Theoretisch-Physikalisches-Institut, Universität Jena,*

*Max-Wien-Platz 1, D-07743 Jena, Germany*

E-mail: wak@tpi.uni-jena.de

The discovery of now about 20 extrasolar planets orbiting solar-type stars with properties quite different from those in our Solar System has raised many questions about the formation and evolution of planets. The tidal interaction between the planet and the surrounding disk determines the orbital properties and the mass of the planet.

We have performed numerical computations of planets embedded in a protoplanetary disk and found that for typical values of the viscosity the planet may easily grow up-to ten Jupiter masses. New results on the mass evolution and the migration of the planet are presented.

## 1. INTRODUCTION

Since the discovery of the first extrasolar planet around a main sequence star five years ago [8] the field of planet searching has grown dramatically. Today about 20 twenty planets of this type are known (for a summary see Marcy, Cochran & Mayor 1999, [7]). The main difference to our own Solar System, where planets have rather small masses and orbit the sun on nearly circular orbits at distances of up-to several AU, has been the discovery of massive planets (up-to 10 Jupiter masses,  $M_{Jup}$ ). Some of the newly discovered planets orbit their central stars very closely (within a tenth of an AU) on orbits with smaller eccentricities. For larger semi-major axis the eccentricities tend to be larger with a maximum of 0.67, see Fig. 1. The only extrasolar planetary system known so far ( $\nu$  And) consists of one planet at 0.059 AU on a nearly circular orbit and two planets at .83 and 2.5 AU having larger eccentricities (.18 and .41) [1]. For a general, up-to date review of the properties of the planets visit the web-site of J. Schneider at <http://www.obspm.fr/planets>.

These rather unexpected findings have brought new momentum into the field of planet formation, and theorists have begun to explore the physical conditions under which planets are supposed to form. It is generally agreed that planets form simultaneously with the star from a collapsing core of an interstellar gas cloud. Angular momentum conservation leads to the formation of a disk where mass is slowly transported inwards and accreted by the star. Some of the material within this accretion disk condenses out to form the planetary embryos which then grow during their final formation stages by rapid accretion of matter from the disk. In

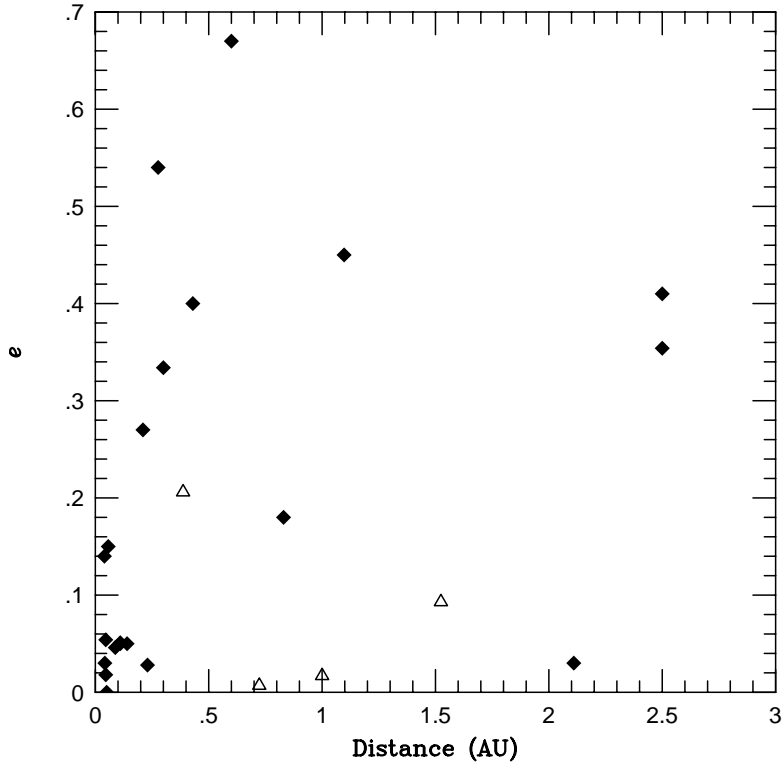


**FIG. 1.** Eccentricity versus semi-major axis for the observed extrasolar planets around main-sequence stars (diamonds) and the inner planets of the Solar System (open triangles). Data are taken from [9].

this scenario all of the newly created planets orbit the stars essentially on circular orbits as they originate from a Keplerian disk, and the more massive, gaseous planets tend to have distances of several AU from the star. While this scenario explains well the observational data of the Solar System, it does not match so well the new results on the extrasolar planets.

As the last phase of planet formation determines the final masses and orbital elements of the planets, it seems fruitful to concentrate in particular on this evolutionary stage. Here we present results of numerical computations of massive (Jupiter type) planets embedded in and evolving simultaneously with the protoplanetary accretion disk.

## 2. MODELING PLANETS IN DISKS

As the vertical thickness of accretion disks is very much smaller than the radial extension, it is well justified to consider only infinitesimally thin disks. Thus, working in cylindrical coordinates, the problem is reduced to two dimensions ( $r - \varphi$ ) where the disk is located in the equatorial plane ( $z = 0$ ), and the origin of the coordinate system is either centered in the middle of the disk or in the center of mass of the system. In this disk a one  $M_{Jup}$  planet is placed initially at a distance of 5.2AU from the one solar mass star, which is the present semi-major axis of Jupiter,  $a_J$ .

The initial surface density profile is given by  $\Sigma \propto r^{-1/2}$  which is the analytic profile for a constant viscosity disk with negligible radial infall velocity. The total mass  $M_d$  in the disk is  $10^{-2}M_\odot$ . At the initial radial location of the planet  $r = a_J$  an annular lowering of the density (gap) is imposed at  $t = 0$  [4]. This speeds up the computations since through the presence of the planet gravitational torques are exerted on the disk which tend to open up an annular gap [5].

Physically, the disk is treated as a viscous fluid with a standard Reynolds stress tensor approximation. The form of the equations for this problem is given for example in Kley (1999) [4]. In these computations we use for simplicity a constant kinematic viscosity which is  $\nu = 10^{-5}$  in dimensionless units, where the unit of distance given by the initial semi-major axis of the planet  $r_0 = 1a_J = 5.2\text{AU}$ , and the unit of time is the inverse Keplerian period  $t_0 = \Omega_k^{-1}(r_0)$  of Jupiter. In the graphics below time is typically given in units of corresponding orbital period  $P = 2\pi t_0$  which is  $11.9\text{yr}$  for Jupiter. The pressure is given by the assumption of a constant vertical disk thickness  $H/r = 0.05$  which is identical to a constant Mach number of 20. We would like to point out that for the given vertical thickness the viscosity corresponds to  $\alpha = 4 \cdot 10^{-3}$ . The basic model parameter are summarized in Table 1.

**TABLE 1**  
The parameter of the standard disk model in which the planets  
are embedded.

Stellar Mass	$1M_\odot$
Disk Mass	$0.01M_\odot$
$H/r$	0.05
Viscosity	$10^{-5}$

Numerically, the combined system of a disk with an embedded planet is modeled by a finite difference method [3] which is second order in space and formally first order in time. Operator splitting is used where the advection and force terms are solved explicitly and the viscous terms implicitly. Typically we use a grid size of  $N_r \times N_\varphi = 128 \times 128$  gridcells which cover a ring-like area from  $r = 0.25 - 4.0$  corresponding to  $1.3 - 20.8\text{AU}$ . Numerical experiments varying for example resolution and the extent of the computational domain (and other numerical parameter) indicate that the major results are not affected by numerical issues [4]. Some of the computations where the planet remains on a fixed circular orbit are performed in the co-rotating frame where the planet is fixed in the grid. Other computations where the planet's orbital parameter are allowed to vary are typically performed in the inertial frame.

### 3. RESULTS

#### 3.1. Fixed orbital parameter of the planet

First we consider the models where the planet was on a fixed circular orbit, which means that the gravitational back-reaction of the disk onto the planet was not taken into account. These models serve to extract the main physical effects an embedded planet experiences within the disk. An overview of the configuration of the standard model (see Table 1) after about 200 orbits of the planet is presented in Fig. 2, where a gray-scale plot of the surface density is presented with lighter

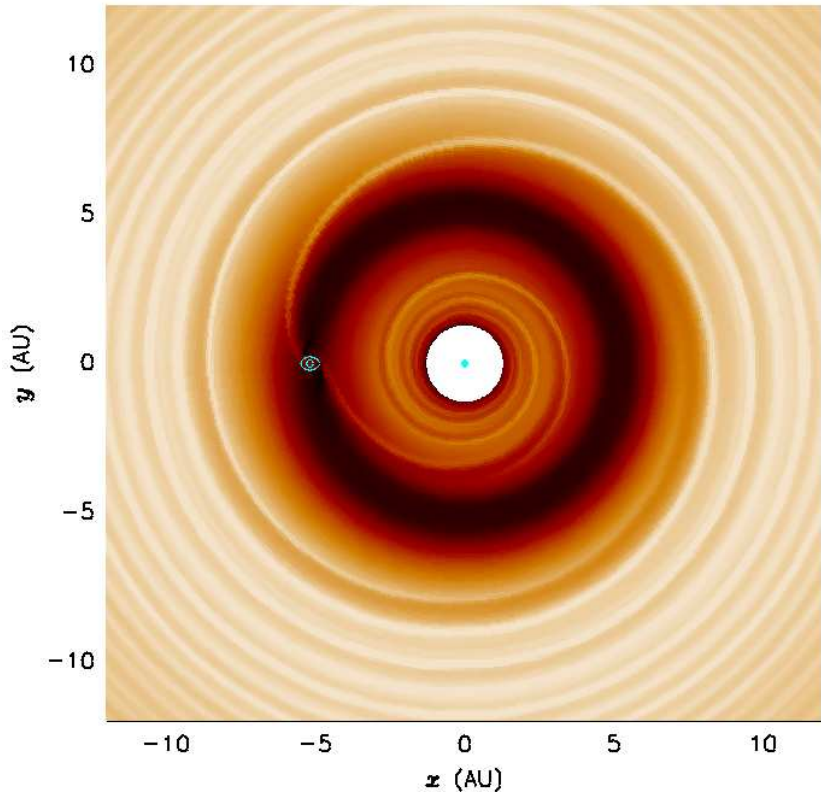


**FIG. 2.** Gray scale plot of the surface density distribution after 200 orbits of the planet, which is located at  $x = -5.2, y = 0.0$ . The white line around the planet indicates its Roche-lobe.

color representing higher density. Clearly visible is the ring-like gap created by the immersed planet where the density is about three orders of magnitude smaller than in the surrounding disc. The gap is formed because the planet acts to extract angular momentum from the inner regions and transports it to the outer which effectively pushes material away from the radial location of the planet. Additionally, there are trailing spiral shock waves induced in the disk. In the regions outside the planet two spiral arms are inter-twined and inside there are three spirals, where one always starts at the location of the planet. The enlargement of the co-rotating flow-field for a higher resolution model (with  $448 \times 128$  gridcells) in the vicinity of the planet, given in Fig. 3, shows the trailing character of the spiral arms. While the material close to  $r = 1$  encircles the star on horseshoe orbits (in the co-rotating frame) some of it enters the Roche-lobe of the planet from upstream region. Mass from both edges, inner and outer, of the gap is able to enter the Roche-lobe.

Assuming that the matter which has entered the planet's Roche-lobe becomes accreted by it, one can estimate the mass accretion rate onto the planet. For a total disk mass of  $10^{-2} M_{\odot}$  this accretion rate is found to be

$$\dot{M}_{pl} = 4.35 \cdot 10^{-5} M_{Jup}/yr$$

which implies a mass doubling timescale for a one Jupiter mass planet of only a few ten thousand years. We note, that this accretion rate onto the planet is larger

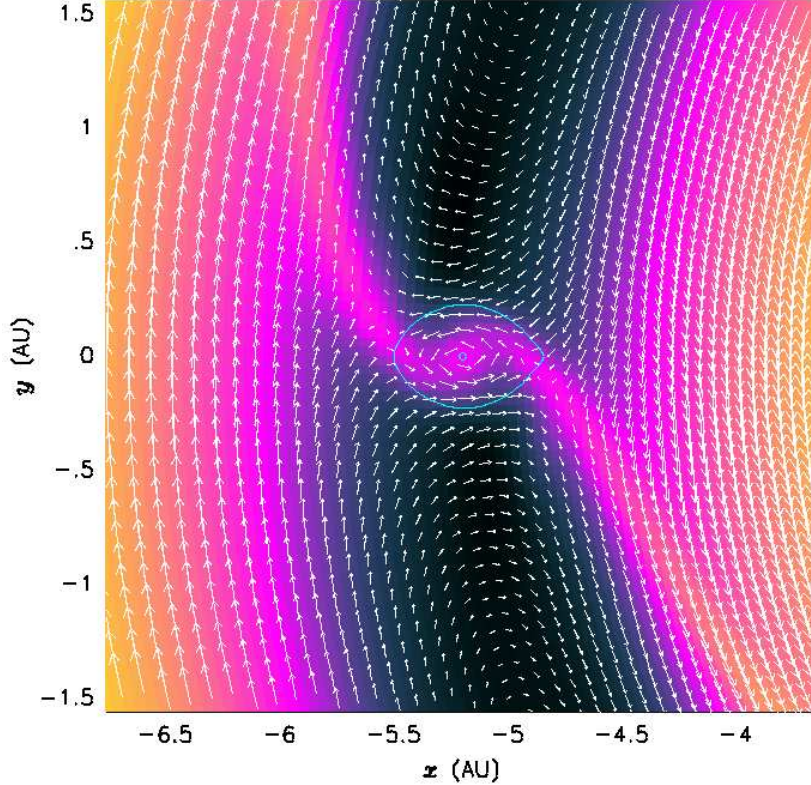


**FIG. 3.** Gray scale plot of the surface density distribution after 200 orbits of the planet, which is located at  $x = -5.2, y = 0.0$ .

than the equilibrium disk accretion rate,  $\dot{M}_{disk} = 3\pi\nu\Sigma$ , which implies that for the given disk parameter all material which is moving viscously inwards will eventually be accreted onto the planet. This gas orbits the planet in the prograde direction in agreement with the observed preferred direction of planetary rotation in the Solar System.

However, the planet can not grow indefinitely since the accretion rate firstly depends on the viscosity and, for values of  $\alpha$  lower than about  $4 \cdot 10^{-4}$  (a value probably not untypical for protostellar disks which are only weakly ionized), it becomes smaller than the disk accretion rate [4, 2]. Additionally, as  $M_{pl}$  increases, the torques exerted by the planet onto the disk grow, that in turn deepens the gap and lowers the accretion rate which is displayed in Fig. 4. Together these mechanisms effectively terminate the mass growth somewhere between 5 and 10  $M_{Jup}$  which is entirely consistent with the observations of extrasolar planets.

### 3.2. Orbital and mass evolution of one planet

The orbital parameter of the planet in the previous calculations were left unchanged even though the disk exerts gravitational torques onto the planet which tend to change those. For a single planet in the disk the change in the semi-major

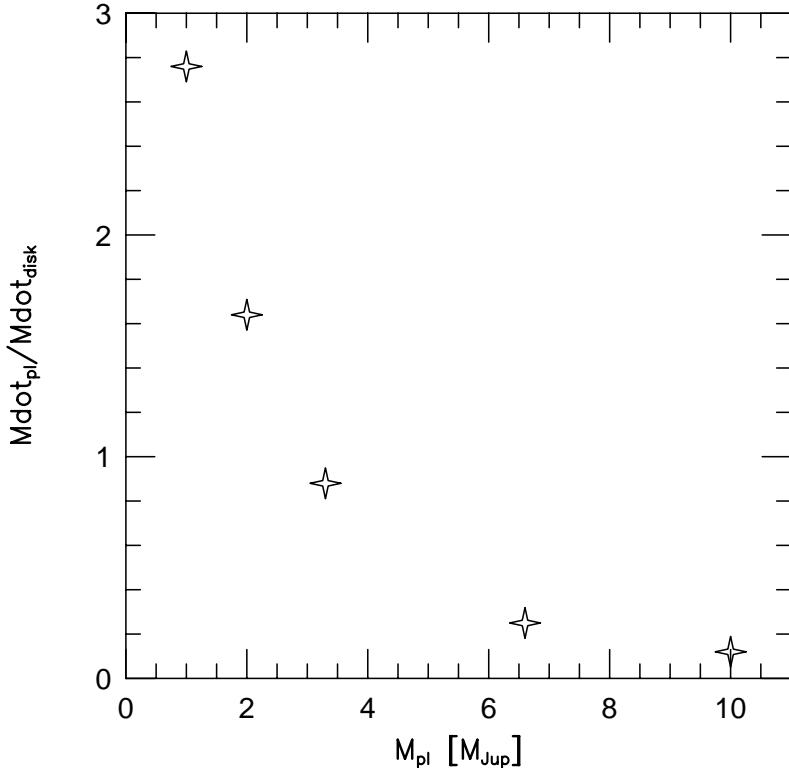


**FIG. 4.** The normalized mass accretion rate  $\dot{M}_{pl}/\dot{M}_{disk}$  onto the planet versus the mass of the planet in units of  $M_{Jup}$ .

axis,  $a$ , may be computed to be

$$\dot{a} = \frac{2}{a M_{pl} \Omega} T_{\perp}$$

where  $T_{\perp}$  is the  $z$ -component of the torque  $\mathbf{T} = \mathbf{r} \times \mathbf{F}$  acting on the planet integrated over the disk's surface. The radial distribution of the torque for the standard model is given in Fig. 5. As the direction of the motion is determined by the sign of the total torque it is clear already from Fig. 5 that the planet will migrate inwards. The main contribution to this lowering of  $a$  comes from the density in trailing spiral arm near the outer edge of the gap. The deep minimum at  $r \approx 1.62$  refers to the  $2 : 1$  outer Lindblad resonance. As the radial inner boundary of the computational domain was open to mass outflow (supposed to have been accreted by the star), the contributions of the regions inside the planets orbit are very small.

The change in the semi-major axis  $\dot{a}$  can be translated into a typical migration timescale

$$\tau_{mig} = \frac{a}{|\dot{a}|}$$

and for the standard model we find that  $\tau_{mig} = 10^5 \text{ yr}$  quite independent of numerical issues. Hence, we do expect a rapid inward migration of the planet, which is displayed in Fig. 6. The inclusion of the variation in the mass of the planet, which

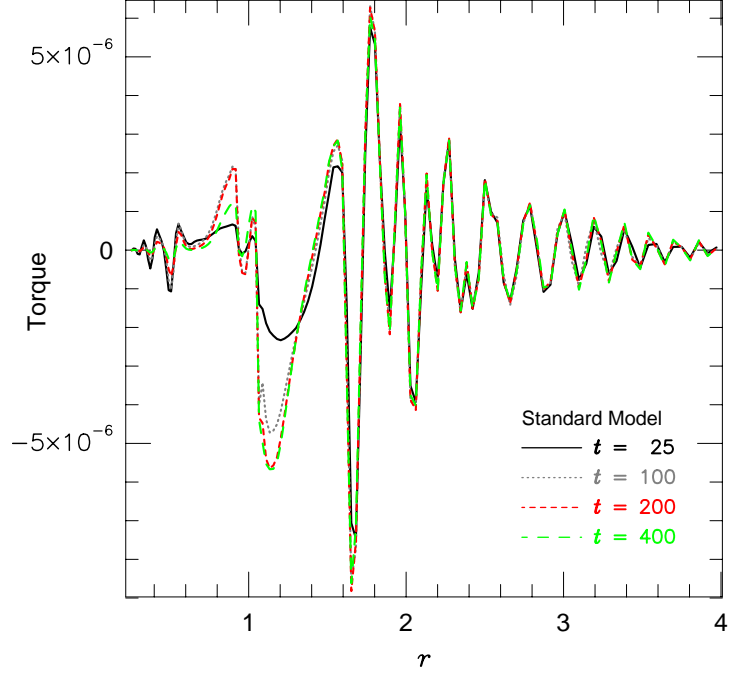


**FIG. 5.** The radial dependence of the azimuthally averaged torque (in dimensionless units) acting on the planet.

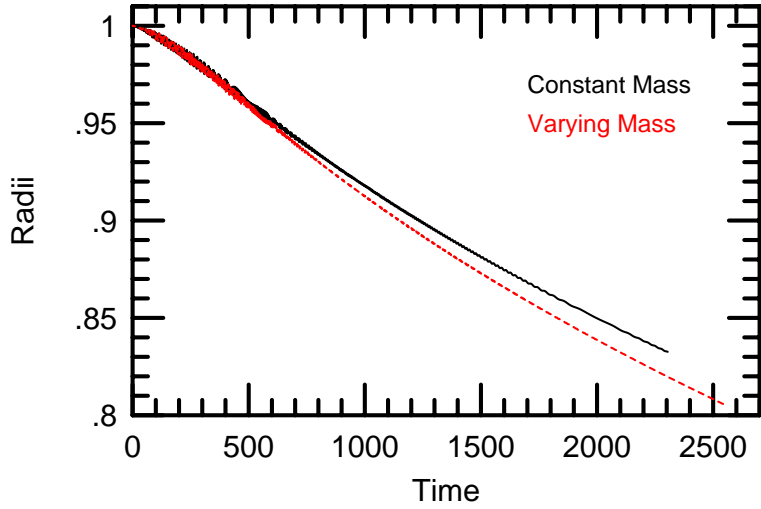


**FIG. 6.** The radial evolution of a migrating planet. In the first model (solid line) the mass of the planet remained fixed while in the second case (dashed) the accreted mass was added to the planet.

has grown to about  $1.8M_{Jup}$  within the 2500 orbits for the second case (dashed line), changes the orbital evolution only slightly. The eccentricity of the planets orbit does not grow during the migration process. However, the migration time scale

becomes longer during the evolution and grows from  $10^5 \text{ yr}$  to nearly  $2 \cdot 10^5 \text{ yr}$  at the end of the computation. By this process of simultaneous inward migration and mass growth one can easily explain the presence of massive planets closely to the central stars which are on nearly circular orbits. In order that the planets do not migrate all the way inwards and are swallowed by the stars a breaking mechanism is required [6]. This may consist of a tidal interaction of the planet with the star, or one may just assume that at some point the mass of the accretion disk is exhausted which terminates the radial evolution in a quite natural way.

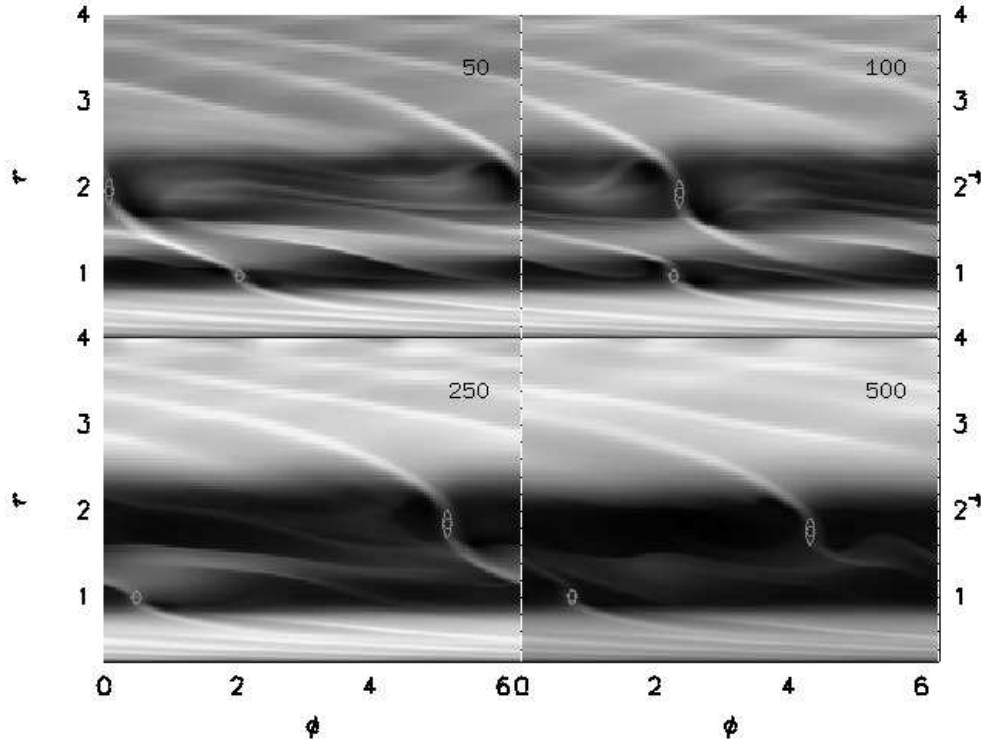


**FIG. 7.** Gray scale plot of the surface density for the two-planet run at four different times, given in units of the initial orbital period of the inner planet. The location of the planets and the sizes of their Roche lobes are indicated.

### 3.3. Evolution of two planets

As it is believed that more eccentric orbits are caused by the interaction of several objects, we have performed a run with two embedded Jupiter-type planets. Initially they were located at  $1a_J$  and  $2a_J$  in opposition to each other, i.e. separated by  $\Delta\varphi = 180^\circ$ . The other physical parameter are identical to the standard model. The system of the two planets and the star is treated as a three body system, where the gravitational back-reaction of the disk on the three objects is fully taken into account. The origin of the coordinate system is fixed in the central star and the equations of motion are integrated using a fourth order Runge-Kutta method. The two planets were assumed to be on circular orbits initially.

Two planets create a much more complicated pattern of wave-like disturbances in the density distribution of the disk than just one planet does. This is displayed

in Fig. 7. In a calculation of one planet on a fixed circular orbit, the wave pattern induced in the disk is stationary in the co-rotating frame. As seen in the plot, here it changes strongly with time. Clearly visible is also the clearing process of mass located initially between the two planets, at about  $t = 500$  one common huge gap has formed. At the same time the inner boundary at  $r = .25a_J$  is open to mass outflow to the star, and the density is reduced in that region.

As both planets accrete basically the mass which enters their Roche-lobes their masses are growing in time but for the inner planet only that gas is available which flows through the gap created by the outer one. Hence the mass of the inner planet grows at a smaller rate than the outer one, see Fig. 8. During the initial gap clearing process the planets grow rapidly in mass and finally reach the asymptotic rates indicated.

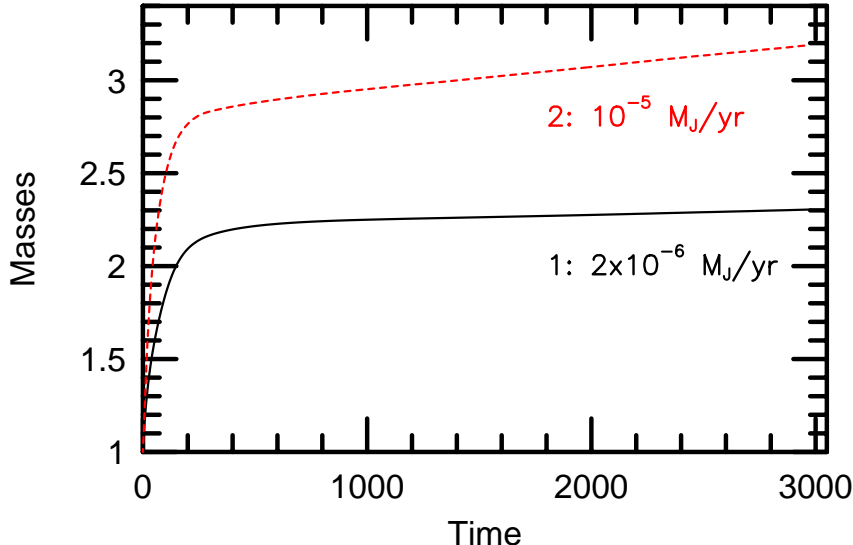


**FIG. 8.** Evolution of the masses of the two planets (1: inner planet, 2: outer planet). The inferred mass accretion rates during the longterm evolution are indicated. Time is given in units of the initial period of the inner planet.

At the same time the gravitational interaction of the two planets, the star and the disk lead to changes in the orbital elements of the objects. The change in the semi-major axis of the planets is given in Fig. 9. The outer planet behaves as in the previous case and migrates slowly inwards. Visible is however, an increase in the eccentricity of the orbit which has grown to about 0.05 at the end of the computation at  $t = 3000$ . The inner planet behaves completely different though: after a very brief initial inward motion it moves outwards and remains there while its eccentricity  $e_2$  grows strongly due to the interaction with the approaching outer planet, reaching  $e_2 = 0.2$  at  $t = 3000$ . The two planets eventually come so close to each other that their orbits are no longer stable and one of them may for example be ejected by the system leaving just one planet on a highly eccentric orbit.

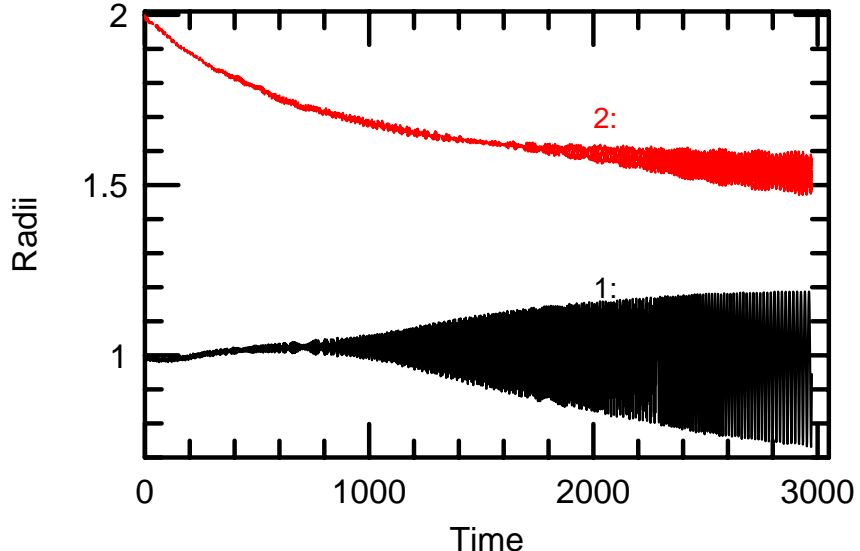


**FIG. 9.** Evolution of the semi-major axis of the two planets. During the evolution the fluctuations of the radial distances to the star strongly increases indicating a growth in eccentricity of the planet.

#### 4. CONCLUSION

We have presented calculations of massive, Jupiter-type planets embedded in protoplanetary disks.

By considering initially one planet on a fixed circular orbit, it was shown that even though the planet opens up an annular gap in disk it is nevertheless able to accrete more mass from its surroundings. As more massive planets induce a wider and deeper gap the mass accumulation basically terminates, which puts the upper limit to the mass of the planet mass at about 5 to 10  $M_{Jup}$ , in good agreement with the observations.

The net gravitational torque of the disk exerted on the planet is generally negative and induces an inward migration of the planet on timescales of about  $t_{mig} \approx 10^5$  yr. During this migration the planet remains essentially on a circular orbit. Using this migration mechanism some basic characteristics (Fig. 1) of the short period extrasolar planets may be explained.

By considering the evolution of a multi-planet system consisting of two Jupiter-type planets we could show that by mutual gravitational interaction the inward motion of the inner planet may come to a halt. As the outer planet approaches the gravitational interaction between the two planets increases which may render their orbits unstable, leading to systems similar to  $\nu$  And. If the protoplanetary nebula has dissipated before the planets come very close to each other one is left with a system of massive planets at several AU distance, similar to our own Solar System.

Through numerical computations which model the interaction between planets and the protoplanetary disk it has been shown that some basic features of the physical parameter (masses, orbital elements) of the observed extrasolar planets may be explainable. To obtain additional insight, more elaborate three-dimensional models which may include radiative effects are required.

### ACKNOWLEDGMENT

Computational resources of the Max-Planck Institute for Astronomy in Heidelberg were available for this project and are gratefully acknowledged. This work was supported by the Max-Planck-Gesellschaft, Grant No. 02160-361-TG74.

### REFERENCES

1. Butler R.P., Marcy G.W., Fischer D.A., Brown T.W., Contos A.R., Korzennik S.G., Nisenson P. & Noyes R.W., 1999, ApJ, in press
2. Bryden G., Chen X., Lin D.N.C, Nelson R.P. & Papaloizou J.C.B., 1999, ApJ, **514**, 344
3. Kley W., 1989, A&A, **208**, 98
4. Kley W., 1999, MNRAS, **303**, 696
5. Lin D.N.C. & Papaloizou J.C.B., 1993, in Levy, E.H., Lunine, J.I., eds, *Protostars and Planets III*, Univ. Arizona Press, Tucson, p749
6. Lin, D.N.C., Bodenheimer, P. & Richardson, D.C., 1996, Nature, **380**, 606.
7. Marcy G.W., Cochran W.D. & Mayor M., 1999, to appear in Mannings V., Boss A. and Russel S. eds, *Protostars and Planets IV*, Univ. Arizona Press, Tucson
8. Mayor M., Queloz D., Nature, 1995, **378**, 355
9. Schneider J., *The Extrasolar Planets Encyclopaedia*, <http://www.obspm.fr/planets>